International Journal for Parasitology: Drugs and Drug Resistance 7 (2017) 191–199

Contents lists available at ScienceDirect

International Journal for Parasitology: Drugs and Drug Resistance

journal homepage: www.elsevier.com/locate/ijpddr

Novel carbazole aminoalcohols as inhibitors of β-hematin formation: Antiplasmodial and antischistosomal activities

Weisi Wang [a, b], Qiang Li [a], Yufen Wei [a], Jian Xue [a], Xiao Sun [c], Yang Yu [c], Zhuo Chen [c], Shizhu Li [a], Liping Duan [a, d, *]

[a] National Institute of Parasitic Diseases, Chinese Center for Disease Control and Prevention, WHO Collaborating Centre for Malaria, Schistosomiasis, and Filariasis, Key Laboratory of Parasitology and Vector Biology of the Chinese Ministry of Health, Shanghai 200025, China
[b] ZJU-ENS Joint Laboratory of Medicinal Chemistry, College of Pharmaceutical Sciences, Zhejiang University, Hangzhou 310058, China
[c] Shanghai Key Laboratory of New Drug Design, School of Pharmacy, East China University of Science and Technology, Shanghai 200237, China
[d] Institute of Microbiology, Chinese Academy of Sciences, Beijing 100101, China

ARTICLE INFO

Article history:
Received 23 September 2016
Received in revised form
29 March 2017
Accepted 29 March 2017
Available online 2 April 2017

Keywords:
Carbazole aminoalcohols
Plasmodium falciparum
Schistosoma japonicum
Antiplasmodials
Antischistosomals
Hematin

ABSTRACT

Malaria and schistosomiasis are two of the most socioeconomically devastating parasitic diseases in tropical and subtropical countries. Since current chemotherapeutic options are limited and defective, there is an urgent need to develop novel antiplasmodials and antischistosomals. Hemozoin is a disposal product formed from the hemoglobin digestion by some blood-feeding parasites. Hemozoin formation is an essential process for the parasites to detoxify free heme, which is a reliable therapeutic target for identifying novel antiparasitic agents. A series of novel carbazole aminoalcohols were designed and synthesized as potential antiplasmodial and antischistosomal agents, and several compounds showed potent *in vitro* activities against *Plasmodium falciparum* 3D7 and Dd2 strains and adult and juvenile *Schistosoma japonicum*. Investigations on the dual antiparasitic mechanisms showed the correlation between inhibitory activity of β-hematin formation and antiparasitic activity. Inhibiting hemozoin formation was identified as one of the mechanisms of action of carbazole aminoalcohols. Compound **7** displayed potent antiplasmodial (*Pf*3D7 IC_{50} = 0.248 μM, *Pf*Dd2 IC_{50} = 0.091 μM) and antischistosomal activities (100% mortality of adult and juvenile schistosomes at 5 and 10 μg/mL, respectively) and exhibited low cytotoxicity (CC_{50} = 7.931 μM), which could be considered as a promising lead for further investigation. Stoichiometry determination and molecular docking studies were also performed to explain the mode of action of compound **7**.

1. Introduction

Parasitic diseases represent a major global health problem. In 2010, the global disability-adjusted life years (DALYs) of parasitic diseases are estimated to be over 102 000, which are greater than some well-known diseases, such as rheumatic heart disease and diabetes (Murray et al., 2012). However, these parasitic diseases are usually "neglected", since they are prevalent mostly in low-income developing countries and poor or marginalized communities. Malaria and schistosomiasis are two typical representatives of these diseases. Most of their current chemotherapeutic strategies suffer from serious deficiencies such as poor efficacy, unacceptable toxicity, high costs and resistance occurrence. Therefore, novel and effective drugs are sorely needed.

Malaria, caused by infection with protozoan of the genus *Plasmodium*, is the most socioeconomically devastating parasitic disease world widely, causing an estimated one million deaths annually (WHO, 2013). Pregnant women and children under five years old are the most affected populations. *Plasmodium falciparum* is the most virulent human malaria parasite, which is responsible for the vast majority of the malaria-related deaths (Nosten et al., 2004). In the absence of effective vaccines, chemotherapy is the important pillar for malaria treatment. However, the global emergence of resistance strains results in the gradual loss of effectiveness of the marketed drugs, including chloroquine, mefloquine and artemisinins (Dondorp et al., 2009).

Schistosomiasis is a chronic and debilitating parasitic disease

* Corresponding author. National Institute of Parasitic Diseases, Chinese Center for Disease Control and Prevention, 207 Ruijin Er Road, Huangpu District, Shanghai 200025, China. Fax: +86 021 64377008 2606.
E-mail address: duanlp1@chinacdc.cn (L. Duan).

http://dx.doi.org/10.1016/j.ijpddr.2017.03.007

caused by blood-flukes of the genus *Schistosoma*. It is the second major parasitic disease in the world after malaria with more than 230 million individuals infected (Gryseels et al., 2006). *Schistosoma japonicum* is the most infectious among the four human pathogenic *Schistosoma* species. (Jia et al., 2007). Schistosomiasis japonica is especially prevalent in lake and marshland regions in Asia, where it still remains significant health concern and considerable economic burden (Garjito et al., 2008; Zhou et al., 2012). Current chemotherapy relies on the only drug, praziquantel, which has been widely used as an effective antischistosomal for decades. Praziquantel is very potent against the adult worms, but much less effective against the juvenile worms (schistosomula) (Fenwick and Webster, 2006). In addition, the adverse effect of mass treatment and long-term medication of praziquantel has revealed available evidence for the emergence of praziquantel resistance in schistosomes (Melman et al., 2009; Pica-Mattoccia et al., 2009). Given the lack of alternative chemotherapeutics, there is a pressing need for new chemical entities for schistosomiasis treatment.

It is known that antiplasmodials have been demonstrated to be able to kill schistosomas *in vitro* and/or *in vivo*, such as artemisinins (Utzinger et al., 2007), mefloquine (Keiser et al., 2010), chloroquine (Oliveira et al., 2004) and pyronaridine (Xue et al., 2013). The detail mechanisms of these drugs exhibiting dual anti-parasitic activity are still unclear. One of the molecular mechanisms involves hemozoin formation (de Villiers and Egan, 2009). Hemozoin is an aggregate of hematin (oxidized heme) produced upon hemoglobin digestion by hematophagous organisms. It is the main mechanism of heme detoxification in several blood-feeding organisms, including *Plasmodium* (Noland et al., 2003), *Schistosoma* (Oliveira et al., 2000), *Haemoproteus columbae* (Chen et al., 2001) and *Rhodnius prolixus* (Stiebler et al., 2010). Free heme (ferriprotoporphyrin IX) is toxic to the parasites, because it can peroxidate lipids, produce oxygen radicals, inhibit enzyme activities and damage cell membranes (Aft and Mueller, 1983, 1984). Hence, how to dispose free heme is of central importance in the physiological processes of hematophagous organisms. To detoxify the free heme, the malaria parasites convert it into insoluble crystals, known as hemozoin. A similar process is observed in schistosomes, and hemozoins are produced and filled in the gut of the worms (Homewood et al., 1972). Since hemozoin formation is essential for the survival of these parasites, inhibiting hematin aggregation represents an attractive drug target. Indeed, plenty of evidence has indicated that antiplasmodial drugs with proved hemozoin formation inhibitory activity were effective for schistosomiasis, e.g. chloroquine (Oliveira et al., 2004), mefloquine (Xiao et al., 2014), and pyronaridine (Auparakkitanon et al., 2006).

In our previous work, a phenotypic *in vitro* screening against adult *S. japonicum* was performed. Among the positive test results, two hits, **JFD03612SC** and **BTB12253SC** (Maybridge database, Fig. 1), arose our interest. Both compounds have a carbazole aminoalcohol scaffold, and caused 100% mortality of adult worms at 10 μg/mL. Besides, further assay results indicated that **JFD03612SC** exhibited moderate antiplasmodial activity against *P. falciparum* 3D7 strain (IC_{50} = 2.671 μM, **BTB12253SC** was not tested). Carbazole occurs in a wide-range of biologically active compounds, including antivirals (Yamada et al., 2012), antibiotics (Hurley et al., 2015), antiplasmodials (Molette et al., 2013). In addition, the aminoalcohol functional group was considered as a privileged structure for antischistosomal activity (Keiser et al., 2009). Thus, we believe that the two hits are good starting points for discovering novel antiparasitic agents against *P. falciparum* and *S. japonicum*.

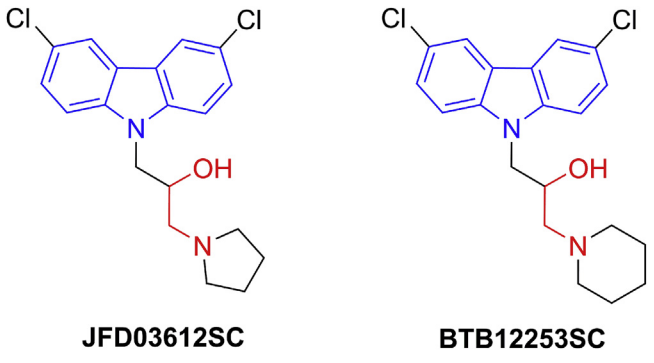

Fig. 1. Chemical structures of two hits.

In this work, sixteen carbazole aminoalcohol derivatives were synthesized to ascertain the importance of the carbazole core, the amine type and the stereochemical structure. Their antiplasmodial activities against *Pf*3D7 and *Pf*Dd2 strains and antischistosomal activities against adult and juvenile *S. japonicum* were determined. Additionally, *β*-hematin formation inhibitory activities of target compounds have also been evaluated. Preliminary structure-activity relationships (SARs) were discussed. Stoichiometry determination and molecular docking studies were carried out, which helped to explain the mode of action of carbazole aminoalcohols.

2. Materials and methods

2.1. General procedures for the synthesis of carbazole aminoalcohols

Reagents and solvents were all purchased from Sigma-Aldrich, and generally were used without further treatment. Melting points were determined in a B-540 Büchi apparatus. NMR spectra were run on a Bruker AM-400 400 MHz spectrometer. Chemical shifts were given in ppm (δ, TMS) and coupling constants in Hz. High resolution mass spectra (HRMS) were recorded on a Thermo Q Exactive Orbitrap LC-MS/MS. Thin layer chromatography (TLC) was performed on silica gel F254 plates from Merck. All yields were unoptimized and generally represented the result of a single experiment.

Synthesis of carbazole aminoalcohols was performed as previously described (Wang et al., 2016a,b). To a solution of 9-(oxiran-2-ylmethyl)-9*H*-carbazole (**2a-c**, 2 mmol) in EtOH (20 mL), corresponding amines (6 mmol) were added. For amines with lower reactivity (e.g. arylamines), $BiCl_3$ (1 mmol) was also added. The reaction mixtures were heated to reflux for 6 h. The progress of the reactions was monitored by TLC. The mixtures were quenched with water (10 mL) and extracted with EtOAc (3 × 10 mL). The organic phases were washed with water (3 × 20 mL) and brine (3 × 20 mL), dried over anhydrous Na_2SO_4, and concentrated under reduced pressure. The obtained residues were purified by recrystallization from ethanol to afford target compounds. The characterization data of compounds **6**–**8** and **12**–**16** were reported in our previous work (Wang et al., 2016a,b), and the characterization data of compounds **3**–**5**, **9**–**11**, **(*R*)-7** and **(*S*)-7)** were given as follows.

2.1.1. 1-(3,6-Dichloro-9H-carbazol-9-yl)-3-(pyrrolidin-1-yl) propan-2-ol (3)

White solid (59%, over two steps), mp: 135.1–137.4 °C. HRMS: m/z = 363.1023 $[M+H]^+$. ^1H NMR (400 MHz, DMSO-d_6) δ 8.30 (d, J = 2.0 Hz, 2H, Ar-H), 7.66 (d, J = 8.8 Hz, 2H, Ar-H), 7.48 (dd, J = 8.8, 2.1 Hz, 2H, Ar-H), 4.96 (d, J = 4.2 Hz, 1H, OH), 4.78–4.26 (m, 2H, CH_2), 4.04–3.97 (m, 1H, CH), 2.56–2.36 (m, 6H, $3CH_2$), 1.73–1.60 (m, 4H, $2CH_2$). ^{13}C NMR (100 MHz, DMSO-d_6) δ 139.77, 125.94, 123.35, 122.37, 120.07, 111.83, 68.32, 59.47, 54.13, 47.58, 23.14.

*2.1.2. 1-(3,6-Dichloro-9H-carbazol-9-yl)-3-(piperidin-1-yl)propan-2-ol **(4)***

White solid (66%, over two steps), mp: 140.3–141.3 °C. HRMS: m/z = 377.1176 $[M+H]^+$. ^{1}H NMR (400 MHz, DMSO-d_6) δ 8.32 (d, J = 2.0 Hz, 2H, Ar-H), 7.67 (d, J = 8.8 Hz, 2H, Ar-H), 7.48 (dd, J = 8.8, 2.0 Hz, 2H, Ar-H), 4.94 (s, 1H, OH), 4.48–4.36 (m, 2H, CH_2), 4.05–3.98 (m, 1H, CH), 2.45–2.24 (m, 6H, $3CH_2$), 1.55–1.34 (m, 6H, $3CH_2$). ^{13}C NMR (100 MHz, DMSO-d_6) δ139.73, 125.92, 123.34, 122.38, 120.12, 111.83, 68.77, 59.77, 54.76, 47.82, 25.61, 23.92.

*2.1.3. 1-(3,6-Dichloro-9H-carbazol-9-yl)-3-morpholinopropan-2-ol **(5)***

White solid (51%, over two steps), mp: 136.3–137.4 °C. HRMS: m/z = 379.0975 $[M+H]^+$. ^{1}H NMR (400 MHz, DMSO-d_6) δ 8.30 (s, 2H, Ar-H), 7.67 (d, J = 8.8 Hz, 2H, Ar-H), 7.48 (dd, J = 8.7 Hz, 2.1 Hz, 2H, Ar-H), 5.00 (d, J = 5.0 Hz, 1H, OH), 4.53–4.21 (m, 2H, CH_2), 4.05 (m, 1H, CH), 3.59–3.53 (m, 4H, $2CH_2$), 2.45–2.25 (m, 6H, $3CH_2$). ^{13}C NMR (100 MHz, DMSO-d_6) δ 139.70, 125.94, 123.36, 122.38, 120.09, 111.83, 66.72, 66.13, 62.10, 54.01, 47.72.

*2.1.4. 1-(3,6-Dichloro-9H-carbazol-9-yl)-3-(hexylamino)propan-2-ol **(9)***

White solid (43%, over two steps), mp: 105.1–107.9 °C. HRMS: m/z = 393.1496 $[M+H]^+$. ^{1}H NMR (400 MHz, DMSO-d_6) δ 8.31 (d, J = 2.0 Hz, 2H, Ar-H), 7.67 (d, J = 8.8 Hz, 2H, Ar-H), 7.47 (dd, J = 8.8, 2.1 Hz, 2H, Ar-H), 5.04 (s, 1H, OH), 4.48–4.19 (m, 2H, CH_2), 3.95–3.93 (m, 1H, CH), 2.57–2.45 (m, 4H, $2CH_2$), 1.41–1.25 (m, 8H, $4CH_2$), 0.86 (t, J = 6.8 Hz, 3H, CH_3). ^{13}C NMR (100 MHz, DMSO-d_6) δ 139.61, 125.92, 123.37, 122.34, 120.10, 111.68, 68.83, 53.13, 49.54, 47.33, 31.28, 29.62, 26.54, 22.11, 13.91.

*2.1.5. 1-(3,6-Dichloro-9H-carbazol-9-yl)-3-(heptylamino)propan-2-ol **(10)***

White solid (63%, over two steps), mp: 74.5–78.1 °C. HRMS: m/z = 407.1645 $[M+H]^+$. ^{1}H NMR (400 MHz, DMSO-d_6) δ 8.31 (d, J = 2.0 Hz, 2H, Ar-H), 7.67 (d, J = 8.8 Hz, 2H, Ar-H), 7.47 (dd, J = 8.8, 2.1 Hz, 2H, Ar-H), 5.03 (s, 1H, OH), 4.48–4.21 (m, 2H, CH_2), 3.95–3.92 (m, 1H, CH), 2.57–2.44 (m, 4H, $2CH_2$), 1.40–1.25 (m, 10H, $5CH_2$), 0.86 (t, J = 6.7 Hz, 3H, CH_3). ^{13}C NMR (100 MHz, DMSO-d_6) δ 139.62, 125.93, 123.37, 122.34, 120.12, 111.71, 68.83, 53.13, 49.53, 47.34, 31.29, 29.65, 28.70, 26.82, 22.08, 13.93.

*2.1.6. 1-(3,6-Dichloro-9H-carbazol-9-yl)-3-(octylamino)propan-2-ol **(11)***

White solid (70%, over two steps), mp: 87.8–91.2 °C. HRMS: m/z = 421.1811 $[M+H]^+$. ^{1}H NMR (400 MHz, DMSO-d_6) δ 8.29 (d, J = 2.0 Hz, 2H, Ar-H), 7.66 (d, J = 8.8 Hz, 2H, Ar-H), 7.45 (dd, J = 8.8, 2.0 Hz, 2H, Ar-H), 4.47–4.23 (m, 2H, CH_2), 3.97–3.92 (m, 1H, CH), 2.57–2.43 (m, 4H, $2CH_2$), 1.38–1.22 (m, 12H, $6CH_2$), 0.84 (t, J = 6.8 Hz, 3H, CH_3). ^{13}C NMR (100 MHz, DMSO-d_6) δ 139.61, 125.91, 123.38, 122.35, 120.10, 111.67, 68.82, 53.11, 49.53, 47.32, 31.29, 29.65, 29.01, 28.74, 26.87, 22.10, 13.92.

*2.1.7. (R)-1-(butylamino)-3-(3,6-dichloro-9H-carbazol-9-yl) propan-2-ol **((R)-7)***

White solid (68%, over two steps), mp: 73.2–75.4 °C. HRMS: m/z = 365.1181 $[M+H]^+$. ^{1}H NMR (400 MHz, DMSO-d_6) δ 8.31 (d, J = 2.1 Hz, 2H, Ar-H), 7.70 (d, J = 8.8 Hz, 2H, Ar-H), 7.48 (dd, J = 8.8, 2.1 Hz, 2H, Ar-H), 4.75–4.61 (m, 1H, OH), 4.48–4.29 (m, 2H, CH_2), 4.05–3.98 (m, 1H, CH), 2.72–2.51 (m, 4H, $2CH_2$), 1.48–1.29 (m, 4H, $2CH_2$), 0.88 (t, J = 7.3 Hz, 3H, CH_3). ^{13}C NMR (100 MHz, DMSO-d_6) δ 139.63, 125.96, 123.37, 122.33, 120.12, 111.74, 68.75, 53.08, 49.12, 47.34, 31.71, 19.93, 13.92.

*2.1.8. (S)-1-(butylamino)-3-(3,6-dichloro-9H-carbazol-9-yl) propan-2-ol **((S)-7)***

White solid (60%, over two steps), mp: 121.5–125.3 °C. HRMS: m/z = 365.1179 $[M+H]^+$. ^{1}H NMR (400 MHz, DMSO-d_6) δ 8.31 (d, J = 2.1 Hz, 2H, Ar-H), 7.68 (d, J = 8.8 Hz, 2H, Ar-H), 7.47 (dd, J = 8.8, 2.1 Hz, 2H, Ar-H), 4.72–4.63 (m, 1H, OH), 4.48–4.26 (m, 2H, CH_2), 3.98–3.93 (m, 1H, CH), 2.59–2.47 (m, 4H, $2CH_2$), 1.43–1.27 (m, 4H, $2CH_2$), 0.88 (t, J = 6.9 Hz, 4H, CH_3). ^{13}C NMR (100 MHz, DMSO-d_6) δ 139.61, 125.98, 123.41, 122.36, 120.14, 111.73, 68.26, 52.57, 48.76, 47.27, 31.02, 19.83, 13.84.

2.2. In vitro P. falciparum whole cell assay

*Pf*3D7 (chloroquine-sensitive) and *Pf*Dd2 (chloroquine-resistant) strains were used in an *in vitro* blood stage culture to evaluate the antiplasmodial efficacy of carbazole aminoalcohols. The strain cultures were prepared following the protocols described by Xu et al. (2013). Intraerythrocytic parasites were synchronised to a 95% ring stage population using 5% sorbitol solution. Chloroquine was dissolved in water (milli-Q grade) to prepare stock solution, and carbazole aminoalcohols and dihydroartemisinin in DMSO. All the stock solutions were diluted with 1640 incomplete medium to reach the corresponding dilutions. Synchronous ring-stage parasites (1% parasitaemia and 2% haematocrit) were incubated in 96-well plates with serial dilutions of test compounds or controls for 72 h at 37 °C. In all cases except chloroquine, the highest final concentration of DMSO was 0.2%, which was found to be nontoxic to the parasites. The antiplasmodial effect of carbazole aminoalcohols was determined by a SYBR Green I fluorometric assay (Xu et al., 2013). IC_{50} values were determined using a growth/sigmoidal option of Origin 8.0.

2.3. In vitro assay for drug effect on adult and juvenile S. japonicum

Adult schistosomes were harvested by dissection from mesenteric veins and livers of infected mice, 34–38 days post-infection. Through perfusion with ice cold Hanks' balanced salt solution (HBSS) containing heparin, schistosomes were collected and rinsed with HBSS three times before incubation. The *in vitro* culture mediums containing RPMI 1640 (with 10% calf serum), 100 IU/mL streptomycin, 100 IU/mL penicillin sodium, and 0.25 g/mL amphotericin B were prepared to maintain the schistosomes. Four pairs of schistosomes (four of both sexes) were placed in each well. The plates were incubated at 37 °C in 5% CO_2 for 2 h. Then test compounds (final drug concentrations: 10 and 5 μg/mL) were added. The final volume of each well was 4.0 mL. DMSO was used as negative control. Phenotypes of the schistosomes, including motility, viability and morphological alterations, were monitored at 24, 48 and 72 h post-incubation. Worm death was defined as no any motor activity observed in suckers and worm bodies for 2 min. No cultured schistosomes were dead in control samples after 72 h incubation.

S. japonicum cercariae were mechanically transformed to schistosomula, and stored in culture medium (RPMI 1640 medium supplemented with 5% fetal bovine serum, 100 IU/mL penicillin and 100 μg/mL streptomycin) at 37 °C in 5% CO_2, as described by Keiser (2010). For drug assay, schistosomula (50/well) were incubated with test compounds (final drug concentration: 10 μg/mL) in a 40-well culture plate at 37 °C in a 5% CO_2 incubator for 72 h. DMSO was used as negative control. Assays were performed in duplicate. The activity status, survival time, mortality and body morphology of the schistosomula were evaluated microscopically at 12 h, 24 h, 48 h and 72 h post-incubation.

2.4. Inhibition assay of β-hematin formation

The inhibition assay of β-hematin was performed using the NP-40 detergent-mediated method (Sandlin et al., 2011). Under acidic experimental conditions, hematin was allowed to form β-hematin. DMSO solution (10 μL) of test compounds at various concentrations was delivered to a 96-well plate, and then 20 μL of NP-40 (30.55 mM) and 70 μL of deionised H_2O were added into each well. The hematin stock solution (25 mM) was prepared by dissolving hematin in DMSO through sonicating, then 178 μL of which was suspended in a 2 M acetate buffer (pH 4.8). For each well, 100 μL of the homogenous suspension was added to reach 0.5 M final buffer and 100 mM hematin. DMSO was used as negative control. Amodiaquine (100 μM, final concentration) was used as a positive control. The plates were covered and incubated at 37 °C for 4 h. Analysis was conducted by using the pyridine-ferrichrome method. A solution of 50% (v/v) pyridine, 20% (v/v) acetone, 30% (v/v) H_2O, and 0.2 M HEPES buffer (pH 7.4) was prepared, and 32 μL of this was delivered to each well to reach a final pyridine concentration of 5% (v/v). In order to give assistance to hematin dispersion, additional acetone (60 μL) was also added. The UV-vis absorbance was recorded by a Bio-Rad Model 680 XR microplate reader at 405 nm. The IC_{50}s of β-hematin formation were determined using GraphPad Prism software. Assays were performed in triplicate, and repeated twice.

2.5. Cytotoxicity assay on WI38 cells

WI38 cells were grown and harvested at log phase. Cells were plated in a 96-well plate at 10 000 cells per well in 180 μL of dulbecco's modified eagle medium (DMEM) or minimal essential medium (MEM) supplemented with 10% fetal bovine serum and 1% penicillin-streptomycin. After 12 h incubation at 37 °C in 5% CO_2 to allow the cells to adhere, 20 μL of 2-fold serial dilutions of compounds were added in the well in triplicate. The final concentrations of compounds were 50, 25, 12.5, 6.25, 3.13 and 1.57 μM. Plates were incubated for another 2 days at 37 °C in 5% CO_2. Then supernatants were removed, and 90 μL of fresh medium and 10 μL of MTT solution were added. After 4 h incubation, the supernatants were removed again and 110 μL of DMSO was added in each well. The plates were swirled gently for 10 min, and then read the absorbance at 490 nm.

2.6. Drug-hematin interaction assay

Stoichiometry determination by the continuous variation method (Job's plot) was carried out to study the drug-hematin interaction through determining the spectral changes. The aqueous DMSO (40%, v/v) solution of 10 M hematin and test compounds were prepared as previously described by Auparakkitanon et al. (2003). The combined concentration of drug and hematin was kept constant (10 μM). For each test drug, 11 solutions of drug and hematin combinations in different molar ratios were prepared as follows: 0:10, 1:9, 1:4, 3:7, 2:3, 1:1, 3:2, 7:3, 4:1, 9:1, and 10:0. Spectra between 240 and 700 nm were read on a Beckman Coulter DU730 spectrophotometer.

2.7. Molecular docking

Docking simulation was performed by using CDOCKER module (Discovery Studio, version 2.1, Accelrys). The three-dimensional structure of heme was obtained from the free heme crystal structure (PDB: 3P5Q). The Fe atom was charged +3, and the Fe (III) protoporphyrin IX form was used for docking simulation. Hemozoin formation occurs within the plasmodium digestive food vacuoles (pH 4.8). At relevant acidic conditions, both N atoms of compound **7** are protonated (Wang et al., 2016a,b). Accordingly, they were charged +1 for docking simulations. For each isomer of **7**, random conformations were generated by utilizing CHARMm field molecular dynamics (1000 steps), and then docked into the defined binding site with a radius set as 11 Å. Other parameters were set as default. The binding conformations of **(*R*)-7** and **(*S*)-7** with heme were determined and ranked according to the calculated CDOCKING energy. Among the top 30 docking poses, the most stable binding modes were showed in Fig. 4. Visualization of docking results was performed with DS Viewer Lite from Accelrys.

3. Results and discussion

3.1. Synthesis of carbazole aminoalcohols

The synthetic routes of carbazole aminoalcohol derivatives are summarized in Fig. 2. Reaction of carbazoles (**1a-c**) and epichlorohydrin (racemic or enantiomerically pure) in the presence of KOH afforded the epoxypropane intermediates (**2a-c**), which subsequently reacted with appropriate amines to obtain corresponding target compounds **3**–**16**.

3.2. Antiplasmodial activity

The *in vitro* antiplasmodial activities of carbazole aminoalcohols were determined against chloroquine-sensitive *Pf*3D7 and chloroquine-resistant *Pf*Dd2 strains. Chloroquine and dihydroartemisinin were used as the positive controls, and the results are summarized in Table 1.

In general, most of the carbazole aminoalcohols exhibited moderate to potent antiplasmodial activities against *Pf*3D7 and *Pf*Dd2 strains. Retaining the dichloronated carbazole core, manipulating the amine tail of **3** altered the activity. All the compounds with alkylamine tails (**6**–**11**) displayed remarkable antiplasmodial activity with IC_{50}s in the submicromolar range against *Pf*3D7 strain and nanomolar range against *Pf*Dd2 strain. Among them, *n*-hexylamino (**9**, *Pf*3D7 IC_{50} = 0.274 μM, *Pf*Dd2 IC_{50} = 0.047 μM) and *n*-octylamino groups (**11**, *Pf*3D7 IC_{50} = 0.132 μM, *Pf*Dd2 IC_{50} = 0.054 μM) were the preferred substituents. For the compounds with aniline substituents (**12**–**14**), a drop of potency was observed. On the other hand, dihalogenated carbazole was found to be a privileged core structure after varying the substituents of carbazole. Comparing with compound **7** (*Pf*3D7 IC_{50} = 0.248 μM, *Pf*Dd2 IC_{50} = 0.091 μM), eliminating the chlorine atoms of carbazole core (**15**, *Pf*3D7 IC_{50} = 0.760 μM, *Pf*Dd2 IC_{50} = 0.334 μM) resulted in 3-fold decrease in potency in both strains. In addition, in order to find out whether the stereochemistry of the secondary hydroxyl group exerted influence on potency, the *R*- and *S*- enantiomers of **7** were prepared and evaluated. Both enantiomers showed similar antiplasmodial activity (**(*R*)-7**, *Pf*3D7 IC_{50} = 0.344 μM, *Pf*Dd2 IC_{50} = 0.172 μM; **(*S*)-7**, *Pf*3D7 IC_{50} = 0.378 μM, *Pf*Dd2 IC_{50} = 0.112 μM).

3.3. Antischistosomal activity

All prepared target compounds were further evaluated for their antischistosomal activity against adult and juvenile *S. japonicum*. The results were summarized in Table 1.

Sixteen compounds were tested, and twelve of them killed all adult *S. japonicum* at 10 μg/mL after 72 h exposure. Among them, seven compounds killed worms with 50–100% mortality at 5 μg/mL. In consistent with the tendency observed in antiplasmodial activity, most of the compounds with alkylamine tails (**6**–**11**) showed significant antischistosomal activity, and the most potent

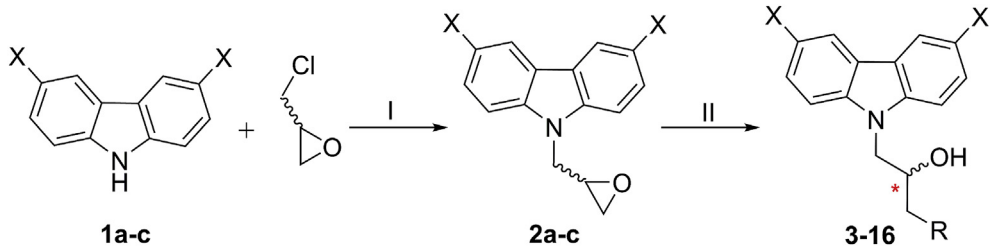

Fig. 2. Synthetic routes of carbazole aminoalcohols. Reagents and conditions: (I) KOH, DMF, 0 °C; (II) amines (RNH_2 or RR'NH), $BiCl_3$, EtOH, reflux.

Table 1
The *in vitro* antiplasmodial, antischistosomal and β-hematin formation inhibitory activities of carbazole aminoalcohols.

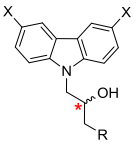

Compd.	X	R	Adult *S. japonicum* worm-killing[a]		Juvenile *S. japonicum* worm-killing[a]	*Pf*3D7 IC_{50} (μM)	*Pf*Dd2 IC_{50} (μM)	β-Hematin	
			10 μg/mL	5 μg/mL	10 μg/mL			% Inhibition[b]	IC_{50} (μM)
3 (JFD03612SC)	Cl		+	−	NT	2.671 ± 0.870	NT	10.76	−
4 (BTB12253SC)	Cl		+	−	NT	NT	NT	NT	−
5	Cl		−	NT	NT	1.294 ± 0.329	NT	0	−
6	Cl		+	±	+	0.379 ± 0.063	0.089 ± 0.015	55.97	151.503 ± 10.454
7	Cl		+	+	+	0.248 ± 0.032	0.091 ± 0.026	82.31	91.839 ± 7.732
8	Cl	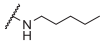	+	±	NT	0.292 ± 0.044	0.121 ± 0.041	48.06	143.820 ± 6.470
9	Cl	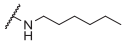	+	±	+	0.274 ± 0.063	0.047 ± 0.010	81.85	54.983 ± 5.872
10	Cl	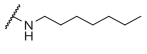	+	±	+	0.179 ± 0.044	0.054 ± 0.010	74.74	91.646 ± 4.667
11	Cl	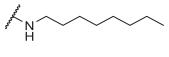	+	±	+	0.132 ± 0.059	0.054 ± 0.006	50.59	65.377 ± 4.899
12	Cl		−	NT	NT	5.404 ± 0.793	NT	0	−
13	Cl		−	NT	NT	4.283 ± 0.684	NT	0	−
14	Cl		−	NT	NT	5.950 ± 0.230	NT	0	−
15	H		+	−	NT	0.760 ± 0.022	0.334 ± 0.067	0	−
16	Br		+	−	NT	0.492 ± 0.100	0.059 ± 0.012	61.51	117.430 ± 8.767
(*R*)-7	Cl		+	+	+	0.344 ± 0.054	0.172 ± 0.032	75.13	118.892 ± 7.136
(*S*)-7	Cl		+	+	+	0.378 ± 0.091	0.112 ± 0.030	80.09	105.517 ± 8.416
Chloroquine	−	−	NT	NT	NT	0.015 ± 0.008	0.231 ± 0.024	97.8	61.011 ± 5.553
Dihydroartemisinin	−	−	NT	NT	NT	NT	0.005 ± 0.0002	NT	NT
Amodiaquine	−	−	NT	NT	NT	NT	NT	100	15.893 ± 1.288
Praziquantel	−	−	+	+	−	−	NT	−	−

NT: not tested.
[a] +: All the cultured *S. japonicum* were dead; −: none of the cultured *S. japonicum* was dead; ±: half of the cultured *S. japonicum* were dead.
[b] % Inhibition assay was performed at a concentration of 100 μM.

compound **7**, with an *n*-butylamino group, killed adult *S. japonicum* with 100% mortality at 5 μg/mL. Both enantiomers of **7**, **(*R*)-7** and **(*S*)-7**, were as effective as the racemate. In accordance with the results of *P. falciparum* whole cell assay, compounds with arylamine substituents (**12**–**14**) suffered a significant loss of potency. In addition, compared with the dichlorinated carbazole derivative **7**, the dibromo- (**15**) and non-substituted (**16**) derivatives exhibited reduced activity against adult worms. Based on the adult worm killing ability, representative compounds were further evaluated for their antischistosomal activity against schistosomula (Table 1). All the tested compounds (**6, 7, 9**–**11**, **(*R*)-7** and **(*S*)-7**) demonstrated significant juvenile worm killing ability, causing 100% mortality at 5 μg/mL in 24 h. The WHO recommended activity criterion of hit compounds for schistosomiasis is 100% inhibition of motility of schistosoma adults at 5 μg/mL (Nwaka and Hudson, 2006). Based on this criterion, compound **7** can be considered for further *in vivo* animal studies.

3.4. β-Hematin formation inhibitory activity

According to the above results, most of the carbazole aminoalcohols showed not only antiplasmodial but also antischistosomal activities, especially those with alkylamine substituents. Plasmodium and schistosome are both hematophagous organisms, and the hemozoin formation is crucial for the survival of these parasites. We speculated that inhibiting hemozoin formation was one of the mechanisms of action of these compounds, similar to the known β-hematin formation inhibitors with dual antiparasitic activities (e.g. chloroquine, mefloquine and pyronaridine). In order to verify our hypothesis, the inhibition assay of β-hematin (synthetic hemozoin) formation was performed. The known inhibitors, chloroquine and amodiaquine, were used as positive controls.

As shown in Table 1, in the preliminary assay, ten compounds showed measurable inhibition ratios at the concentration of 100 μM. The presence of an alkylamine tail (**6**–**11**) was favorable to potency. Compounds with alicyclic amine groups (**3** and **5**) or arylamine groups (**12**–**14**) were not able to inhibit β-hematin formation. The removal of two halogens on the carbazole moiety (**15**) resulted in a dramatic decrease in potency, which demonstrated the essential role of dihalogen-substituted carbazole core. Further assay results indicated that almost all the compounds possessing alkylamine groups (**6**–**11**) exhibited significant β-hematin formation inhibitory activity. Especially, compounds with *n*-butylamino (**7**, IC_{50} = 91.839 μM), *n*-hexylamino (**9**, IC_{50} = 54.983 μM), *n*-heptylamino (**10**, IC_{50} = 91.646 μM), and *n*-octylamino (**11**, IC_{50} = 65.377 μM) groups displayed potent activity equivalent to that of chloroquine (IC_{50} = 61.01 μM). The stereochemistry of the linker had no influence on potency.

The antiplasmodial activity of carbazole aminoalcohols have been identified in several phenotypic screenings, but their mode of action remains unclear. Recently, it has been reported that *Plasmodium falciparum* Hsp90 was a plausible target of carbazole aminoalcohols (Wang et al., 2016a,b), while there is still no clue of their mechanism of action on schistosomes. In this work, three kinds of biological assay revealed a similar SAR pattern: (1) dichlorinated carbazole acted as a privileged core; (2) an alkylamine tail was beneficial for activity; conversely, arylamine substituents imparted negative effect to potency; and (3) stereochemistry of the secondary hydroxyl group had no influence on potency. The SARs indicated that β-hematin formation inhibitory activity of target compounds showed correlation with their antiplasmodial and antischistosomal activities, especially the latter. Although further investigations are needed, the current data basically confirmed our hypothesis that inhibiting hemozoin formation was one of the mechanisms of action of carbazole aminoalcohols.

3.5. Cytotoxicity

In order to assess the toxicity of carbazole aminoalcohols, representative compounds (**6**–**11**) were tested for their cytotoxicity against human embryonic lung fibroblast WI38. The results were summarized in Table 2 (CC_{50}s). Generally, all of the tested compounds showed moderate cytotoxicity with CC_{50}s in the micromolar range. The selectivity indices (SI), the ratio of cytotoxicity (CC_{50}) and antiplasmodial activity (IC_{50} for *Pf* strains), were also calculated (Table 2), allowing to identify the potential therapeutic windows. All the compounds showed acceptable SI values in chloroquine-sensitive *Pf*3D7 strain ranging from 19 to 32, and more satisfactory SI were observed in chloroquine-resistant *Pf*Dd2 strain ranging from 45 to 126 (Table 1). Particularly, compound **7** was the safest molecule with a CC_{50} value of 7.931 μM, a SI [CC_{50}/IC_{50} (*Pf*3D7)] value of 32, and a SI [CC_{50}/IC_{50} (*Pf*Dd2)] value of 87.

3.6. Stoichiometry determination by the continuous variation method (Job's plot)

The binding of carbazole aminoalcohols with hematin was investigated by the continuous variation technique (Job's plot). A sharp peak at 401 nm was observed in hematin solution at pH 7.4, indicating that monomeric hematin predominated under the experimental conditions. The addition of represented carbazole aminoalcohols (**6**–**11**) led to the decrease of absorption in the Soret band, indicating the association of compounds and hematin. When the molar ratios of hematin and compounds were 1:1, changes in absorbance intensity reached the maximum (see Fig. 3 for representative plot of **7**). It demonstrated the formation of a 1:1 drug:hematin complex. In contrast with **7** and **9**, compounds **6** and **8** produced minor changes in absorbance (data not shown), suggesting that they interacted weakly with hematin, which was in agreement with their less potent β-hematin formation inhibitory activity.

3.7. Molecular docking studies

Molecular docking studies were performed to predict the binding modes of representative compound **7** (*R* and *S* isomers) with heme by utilizing the C-DOCKER program within Discovery Studio 2.1 software package.

As expected, the docking models (Fig. 4) indicated that **(*R*)-7** and **(*S*)-7** exhibited similar binding modes with heme. Both isomers could form stable non-covalent complexes with heme, which consequently led to the inhibition of hemozoin formation. As observed from the axial view (Fig. 4a and b), the carbazole core formed a π-π stacking interaction with porphyrin ring. It probably played a key role in the stability of drug-heme complex. The

Table 2
The *in vitro* cytotoxicity and selectivity indices of carbazole aminoalcohols.

Compd.	CC_{50} (μM)[a]	SI[b]	
		CC_{50}/IC_{50} (*Pf*3D7)	CC_{50}/IC_{50} (*Pf*Dd2)
6	7.268	19	82
7	7.931	32	87
8	6.259	21	52
9	5.920	22	126
10	5.141	28	95
11	3.773	29	70
(*R*)-7	7.686	22	45
(*S*)-7	9.343	24	83

[a] 50% Cytotoxic concentration, WI38 cell line, means of two independent experiments.
[b] Selectivity Index (SI) was calculated as CC_{50}/IC_{50} ratio.

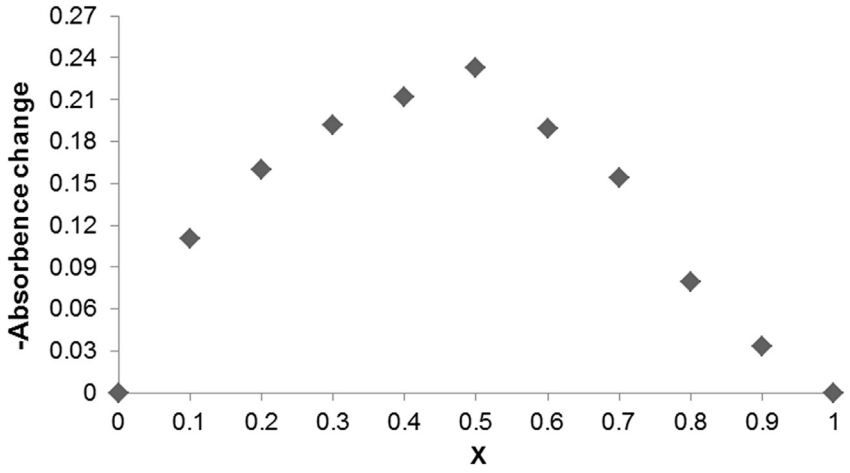

Fig. 3. Job's plot of carbazole aminoalcohol derivative **7** binding to hematin. X means the mole fraction of **7**, x = [**7**]/[**7**]+[hematin].

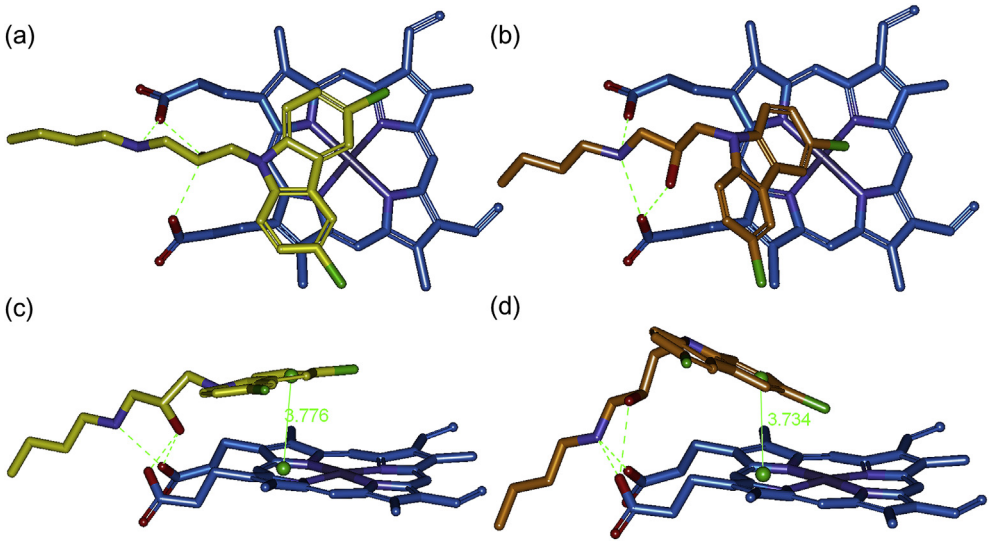

Fig. 4. Molecular docking results for: (a) (***R***)**-7** and heme, axial view; (b) (***S***)**-7** and heme, axial view; (c) (***R***)**-7** and heme, side view; (d) (***S***)**-7** and heme, side view. Protons were omitted for clarity. Backbone color code: yellow for (***R***)**-7**, orange for (***S***)**-7** and blue for heme. The interplanar distances between carbazole centroid and porphyrin ring were measured and labeled with green solid lines. H-bonds were highlighted as green dashes. (For interpretation of the references to colour in this figure legend, the reader is referred to the web version of this article.)

carbazole core was not right above the iron center, but located toward one side of porphyrin ring, presumably to form preferable π-π interaction. Similar binding modes were observed in amodiaquine-, chloroquine-, and quinine-heme complexes (Leed et al., 2002; de Dios et al., 2004). The aminoalcohol functional groups (NH and OH) of (***R***)**-7** and (***S***)**-7** formed three hydrogen bonds with both carboxyls of heme, respectively, which probably further stabilized the complex. The side view (Fig. 4c and d) showed that the distances between carbazole centroid and heme porphyrin planar of (***R***)**-7** and (***S***)**-7** were 3.78 and 3.73 Å, respectively, which satisfied the optimal interplanar distance value of approximate 3.0–4.0 Å (de Sousa et al., 2015).

4. Conclusions

In this work, novel carbazole aminoalcohols were designed and prepared, and their antiplasmodial and antischistosomal potential have been confirmed. Most of the compounds displayed significant β-hematin formation inhibitory ability, which showed correlation with their dual antiparasitic activities, identifying that inhibiting hemozoin formation was one of their mechanisms of action. The preliminary SARs confirmed the importance of the amine type and the dichlorinated carbazole core. Job's plot revealed that carbazole aminoalcohol compound interacted with hematin through forming a 1:1 complex. It is noteworthy that compound **7** showed not only potent dual antiparasitic activities but also low cytotoxicity, which could be developed as a promising lead compound for further investigation.

Acknowledgments

This work was supported by China Postdoctoral Science Foundation funded project (grant number 2015M571147), the National Natural Science Foundation of China (grant numbers 21502181 and 21302054), Shanghai Municipal Commission of Health and Family Planning funded project (grant number 201440537) and the project of echinococcosis prevention and control - Ganzi workstation.

References

Aft, R.L., Mueller, G.C., 1983. Hemin-mediated DNA strand scission. J. Biol. Chem. 258, 12069–12072.

Aft, R.L., Mueller, G.C., 1984. Hemin-mediated oxidative degradation of proteins. J. Biol. Chem. 259, 301–305.

Auparakkitanon, S., Noonpakdee, W., Ralph, R.K., Denny, W.A., Wilairat, P., 2003. Antimalarial 9-anilinoacridine compounds directed at hematin. Antimicrob. Agents Chemother. 47, 3708–3712.

Auparakkitanon, S., Chapoomram, S., Kuaha, K., Chirachariyavej, T., Wilairat, P., 2006. Targeting of hematin by the antimalarial pyronaridine. Antimicrob. Agents Chemother. 50, 2197–2200.

Chen, M.M., Shi, L., Sullivan, D.J., 2001. *Haemoproteus* and *Schistosoma* synthesize heme polymers similar to *Plasmodium* hemozoin and β-hematin. Mol. Biochem. Parasitol. 113, 1–8.

de Dios, A.C., Casabianca, L.B., Kosar, A., Roepe, P.D., 2004. Structure of the amodiaquine-FPIX μ-oxo-dimer solution complex at atomic resolution. Inorg. Chem. 43, 8078–8084.

de Sousa, A.C.C.E., Diaz, N.C., de Souza, A.M.C.C., Cabral, L.U.C.M., Castro, H.C., Albuquerque, M.G.A.O., Rodrigues, C.R., 2015. Molecular modeling study of a series of amodiaquine analogues with antimalarial activity. Med. Chem. Res. 24, 3529–3536.

de Villiers, K.A., Egan, T.J., 2009. Recent advances in the discovery of haem-targeting drugs for malaria and schistosomiasis. Molecules 14, 2868–2887.

Dondorp, A.M., Nosten, F., Yi, P., Das, D., Phyo, A.P., Tarning, J., Lwin, K.M., Ariey, F., Hanpithakpong, W., Lee, S.J., Ringwald, P., Silamut, K., Imwong, M., Chotivanich, K., Lim, P., Herdman, T., An, S.S., Yeung, S., Singhasivanon, P., Day, N.P.J., Lindegardh, N., Socheat, D., White, N.J., 2009. Artemisinin resistance in *Plasmodium falciparum* malaria. N. Engl. J. Med. 361, 455–467.

Fenwick, A., Webster, J.P., 2006. Schistosomiasis: challenges for control, treatment and drug resistance. Curr. Opin. Infect. Dis. 19, 577–582.

Garjito, T.A., Sudomo, M., Abdullah, Dahlan, M., Nurwidayati, A., 2008. Schistosomiasis in Indonesia: past and present. Parasitol. Int. 57, 277–280.

Gryseels, B., Polman, K., Clerinx, J., Kestens, L., 2006. Human schistosomiasis. Lancet 368, 1106–1118.

Homewood, C.A., Jewsbury, J.M., Chance, M.L., 1972. The pigment formed during haemoglobin digestion by malarial and schistosomal parasites. Comp. Biochem. Physiol. B 43, 517–523.

Hurley, K.A., Heinrich, V.A., Hershfield, J.R., Demons, S.T., Weibel, D.B., 2015. Membrane-targeting DCAP analogues with broad-spectrum antibiotic activity against pathogenic bacteria. Acs Med. Chem. Lett. 6, 466–471.

Jia, T.W., Zhou, X.N., Wang, X.H., Utzinger, J., Steinmann, P., Wu, X.H., 2007. Assessment of the age-specific disability weight of chronic schistosomiasis japonica. Bull. World Health Organ 85, 458–465.

Keiser, J., Chollet, J., Xiao, S.H., Mei, J.Y., Jiao, P.Y., Utzinger, J., Tanner, M., 2009. Mefloquine–an aminoalcohol with promising antischistosomal properties in mice. PLoS Negl. Trop. Dis. 3, e350.

Keiser, J., N'Guessan, N.A., Adoubryn, K.D., Silue, K.D., Vounatsou, P., Hatz, C., Utzinger, J., N'Goran, E.K., 2010. Efficacy and safety of mefloquine, artesunate, mefloquine-artesunate, and praziquantel against *Schistosoma haematobium*: randomized, exploratory open-label trial. Clin. Infect. Dis. 50, 1205–1213.

Keiser, J., 2010. *In vitro* and *in vivo* trematode models for chemotherapeutic studies. Parasitology 137, 589–603.

Leed, A., DuBay, K., Ursos, L.M., Sears, D., De Dios, A.C., Roepe, P.D., 2002. Solution structures of antimalarial drug-heme complexes. Biochemistry-Us 41, 10245–10255.

Melman, S.D., Steinauer, M.L., Cunningham, C., Kubatko, L.S., Mwangi, I.N., Wynn, N.B., Mutuku, M.W., Karanja, D.M., Colley, D.G., Black, C.L., Secor, W.E., Mkoji, G.M., Loker, E.S., 2009. Reduced susceptibility to praziquantel among naturally occurring Kenyan isolates of *Schistosoma mansoni*. PLoS Negl. Trop. Dis. 3, e504.

Molette, J., Routier, J., Abla, N., Besson, D., Bombrun, A., Brun, R., Burt, H., Georgi, K., Kaiser, M., Nwaka, S., Muzerelle, M., Scheer, A., 2013. Identification and optimization of an aminoalcohol-carbazole series with antimalarial properties. Acs Med. Chem. Lett. 4, 1037–1041.

Murray, C.J., Vos, T., Lozano, R., Naghavi, M., Flaxman, A.D., Michaud, C., Ezzati, M., Shibuya, K., Salomon, J.A., Abdalla, S., Aboyans, V., Abraham, J., Ackerman, I., Aggarwal, R., Ahn, S.Y., Ali, M.K., Alvarado, M., Anderson, H.R., Anderson, L.M., Andrews, K.G., Atkinson, C., Baddour, L.M., Bahalim, A.N., Barker-Collo, S., Barrero, L.H., Bartels, D.H., Basanez, M.G., Baxter, A., Bell, M.L., Benjamin, E.J., Bennett, D., Bernabe, E., Bhalla, K., Bhandari, B., Bikbov, B., Bin, A.A., Birbeck, G., Black, J.A., Blencowe, H., Blore, J.D., Blyth, F., Bolliger, I., Bonaventure, A., Boufous, S., Bourne, R., Boussinesq, M., Braithwaite, T., Brayne, C., Bridgett, L., Brooker, S., Brooks, P., Brugha, T.S., Bryan-Hancock, C., Bucello, C., Buchbinder, R., Buckle, G., Budke, C.M., Burch, M., Burney, P., Burstein, R., Calabria, B., Campbell, B., Canter, C.E., Carabin, H., Carapetis, J., Carmona, L., Cella, C., Charlson, F., Chen, H., Cheng, A.T., Chou, D., Chugh, S.S., Coffeng, L.E., Colan, S.D., Colquhoun, S., Colson, K.E., Condon, J., Connor, M.D., Cooper, L.T., Corriere, M., Cortinovis, M., de Vaccaro, K.C., Couser, W., Cowie, B.C., Criqui, M.H., Cross, M., Dabhadkar, K.C., Dahiya, M., Dahodwala, N., Damsere-Derry, J., Danaei, G., Davis, A., De Leo, D., Degenhardt, L., Dellavalle, R., Delossantos, A., Denenberg, J., Derrett, S., Des Jarlais, D.C., Dharmaratne, S.D., Dherani, M., Diaz-Torne, C., Dolk, H., Dorsey, E.R., Driscoll, T., Duber, H., Ebel, B., Edmond, K., Elbaz, A., Ali, S.E., Erskine, H., Erwin, P.J., Espindola, P., Ewoigbokhan, S.E., Farzadfar, F., Feigin, V., Felson, D.T., Ferrari, A., Ferri, C.P., Fevre, E.M., Finucane, M.M., Flaxman, S., Flood, L., Foreman, K., Forouzanfar, M.H., Fowkes, F.G., Fransen, M., Freeman, M.K., Gabbe, B.J., Gabriel, S.E., Gakidou, E., Ganatra, H.A., Garcia, B., Gaspari, F., Gillum, R.F., Gmel, G., Gonzalez-Medina, D., Gosselin, R., Grainger, R., Grant, B., Groeger, J., Guillemin, F., Gunnell, D., Gupta, R., Haagsma, J., Hagan, H., Halasa, Y.A., Hall, W., Haring, D., Haro, J.M., Harrison, J.E., Havmoeller, R., Hay, R.J., Higashi, H., Hill, C., Hoen, B., Hoffman, H., Hotez, P.J., Hoy, D., Huang, J.J., Ibeanusi, S.E., Jacobsen, K.H., James, S.L., Jarvis, D., Jasrasaria, R., Jayaraman, S., Johns, N., Jonas, J.B., Karthikeyan, G., Kassebaum, N., Kawakami, N., Keren, A., Khoo, J.P., King, C.H., Knowlton, L.M., Kobusingye, O., Koranteng, A., Krishnamurthi, R., Laden, F., Lalloo, R., Laslett, L.L., Lathlean, T., Leasher, J.L., Lee, Y.Y., Leigh, J., Levinson, D., Lim, S.S., Limb, E., Lin, J.K., Lipnick, M., Lipshultz, S.E., Liu, W., Loane, M., Ohno, S.L., Lyons, R., Mabweijano, J., MacIntyre, M.F., Malekzadeh, R., Mallinger, L., Manivannan, S., Marcenes, W., March, L., Margolis, D.J., Marks, G.B., Marks, R., Matsumori, A., Matzopoulos, R., Mayosi, B.M., McAnulty, J.H., McDermott, M.M., McGill, N., McGrath, J., Medina-Mora, M.E., Meltzer, M., Mensah, G.A., Merriman, T.R., Meyer, A.C., Miglioli, V., Miller, M., Miller, T.R., Mitchell, P.B., Mock, C., Mocumbi, A.O., Moffitt, T.E., Mokdad, A.A., Monasta, L., Montico, M., Moradi-Lakeh, M., Moran, A., Morawska, L., Mori, R., Murdoch, M.E., Mwaniki, M.K., Naidoo, K., Nair, M.N., Naldi, L., Narayan, K.M., Nelson, P.K., Nelson, R.G., Nevitt, M.C., Newton, C.R., Nolte, S., Norman, P., Norman, R., O'Donnell, M., O'Hanlon, S., Olives, C., Omer, S.B., Ortblad, K., Osborne, R., Ozgediz, D., Page, A., Pahari, B., Pandian, J.D., Rivero, A.P., Patten, S.B., Pearce, N., Padilla, R.P., Perez-Ruiz, F., Perico, N., Pesudovs, K., Phillips, D., Phillips, M.R., Pierce, K., Pion, S., Polanczyk, G.V., Polinder, S., Pope, C.R., Popova, S., Porrini, E., Pourmalek, F., Prince, M., Pullan, R.L., Ramaiah, K.D., Ranganathan, D., Razavi, H., Regan, M., Rehm, J.T., Rein, D.B., Remuzzi, G., Richardson, K., Rivara, F.P., Roberts, T., Robinson, C., De Leon, F.R., Ronfani, L., Room, R., Rosenfeld, L.C., Rushton, L., Sacco, R.L., Saha, S., Sampson, U., Sanchez-Riera, L., Sanman, E., Schwebel, D.C., Scott, J.G., Segui-Gomez, M., Shahraz, S., Shepard, D.S., Shin, H., Shivakoti, R., Singh, D., Singh, G.M., Singh, J.A., Singleton, J., Sleet, D.A., Sliwa, K., Smith, E., Smith, J.L., Stapelberg, N.J., Steer, A., Steiner, T., Stolk, W.A., Stovner, L.J., Sudfeld, C., Syed, S., Tamburlini, G., Tavakkoli, M., Taylor, H.R., Taylor, J.A., Taylor, W.J., Thomas, B., Thomson, W.M., Thurston, G.D., Tleyjeh, I.M., Tonelli, M., Towbin, J.A., Truelsen, T., Tsilimbaris, M.K., Ubeda, C., Undurraga, E.A., van der Werf, M.J., van Os, J., Vavilala, M.S., Venketasubramanian, N., Wang, M., Wang, W., Watt, K., Weatherall, D.J., Weinstock, M.A., Weintraub, R., Weisskopf, M.G., Weissman, M.M., White, R.A., Whiteford, H., Wiebe, N., Wiersma, S.T., Wilkinson, J.D., Williams, H.C., Williams, S.R., Witt, E., Wolfe, F., Woolf, A.D., Wulf, S., Yeh, P.H., Zaidi, A.K., Zheng, Z.J., Zonies, D., Lopez, A.D., AlMazroa, M.A., Memish, Z.A., 2012. Disability-adjusted life years (DALYs) for 291 diseases and injuries in 21 regions, 1990-2010: a systematic analysis for the Global Burden of Disease Study 2010. Lancet 380, 2197–2223.

Noland, G.S., Briones, N., Sullivan, D.J., 2003. The shape and size of hemozoin crystals distinguishes diverse *Plasmodium* species. Mol. Biochem. Parasitol. 130, 91–99.

Nosten, F., Rogerson, S.J., Beeson, J.G., McGready, R., Mutabingwa, T.K., Brabin, B., 2004. Malaria in pregnancy and the endemicity spectrum: what can we learn? Trends Parasitol. 20, 425–432.

Nwaka, S., Hudson, A., 2006. Innovative lead discovery strategies for tropical diseases. Nat. Rev. Drug Discov. 5, 941–955.

Oliveira, M.F., D'Avila, J.C., Torres, C.R., Oliveira, P.L., Tempone, A.J., Rumjanek, F.D., Braga, C.M., Silva, J.R., Dansa-Petretski, M., Oliveira, M.A., de Souza, W., Ferreira, S.T., 2000. Haemozoin in *Schistosoma mansoni*. Mol. Biochem. Parasitol. 111, 217–221.

Oliveira, M.F., D'Avila, J.C., Tempone, A.J., Soares, J.B., Rumjanek, F.D., Ferreira-Pereira, A., Ferreira, S.T., Oliveira, P.L., 2004. Inhibition of heme aggregation by chloroquine reduces *Schistosoma mansoni* infection. J. Infect Dis 190, 843–852.

Pica-Mattoccia, L., Doenhoff, M.J., Valle, C., Basso, A., Troiani, A.R., Liberti, P., Festucci, A., Guidi, A., Cioli, D., 2009. Genetic analysis of decreased praziquantel sensitivity in a laboratory strain of *Schistosoma mansoni*. Acta Trop. 111, 82–85.

Sandlin, R.D., Carter, M.D., Lee, P.J., Auschwitz, J.M., Leed, S.E., Johnson, J.D., Wright, D.W., 2011. Use of the NP-40 detergent-mediated assay in discovery of inhibitors of β-hematin crystallization. Antimicrob. Agents Chemother. 55, 3363–3369.

Stiebler, R., Timm, B.L., Oliveira, P.L., Hearne, G.R., Egan, T.J., Oliveira, M.F., 2010. On the physico-chemical and physiological requirements of hemozoin formation promoted by perimicrovillar membranes in *Rhodnius prolixus* midgut. Insect Biochem. Mol. Biol. 40, 284–292.

Utzinger, J., Xiao, S.H., Tanner, M., Keiser, J., 2007. Artemisinins for schistosomiasis and beyond. Curr. Opin. Investig. Drugs 8, 105–116.

Wang, T., Maser, P., Picard, D., 2016a. Inhibition of *Plasmodium falciparum* Hsp90 contributes to the antimalarial activities of aminoalcohol-carbazoles. J. Med. Chem. 59, 6344–6352.

Wang, W., Sun, X., Sun, D., Li, S., Yu, Y., Yang, T., Yao, J., Chen, Z., Duan, L., 2016b. Carbazole aminoalcohols induce antiproliferation and apoptosis of human tumor cells by inhibiting topoisomerase I. Chemmedchem 11, 2675–2681.

WHO, 2013. World Malaria Report. http://www.who.int/malaria/publications/world_malaria_report_2013/report/en/.

Xiao, S.H., Qiao, C., Xue, J., Wang, L., 2014. Mefloquine in combination with hemin causes severe damage to adult *Schistosoma japonicum in vitro*. Acta Trop. 131, 71–78.

Xu, M., Zhu, J., Diao, Y., Zhou, H., Ren, X., Sun, D., Huang, J., Han, D., Zhao, Z., Zhu, L.,

Xu, Y., Li, H., 2013. Novel selective and potent inhibitors of malaria parasite dihydroorotate dehydrogenase: discovery and optimization of dihydrothiophenone derivatives. J. Med. Chem. 56, 7911–7924.

Xue, J., Jiang, B., Liu, C.S., Sun, J., Xiao, S.H., 2013. Comparative observation on inhibition of hemozoin formation and their *in vitro* and *in vivo* anti-schistosome activity displayed by 7 antimalarial drugs. Chin. J. Parasitol. Parasit. Dis. 31, 161–169.

Yamada, K., Koyama, H., Hagiwara, K., Ueda, A., Sasaki, Y., Kanesashi, S.N., Ueno, R., Nakamura, H.K., Kuwata, K., Shimizu, K., Suzuki, M., Aida, Y., 2012. Identification of a novel compound with antiviral activity against influenza A virus depending on PA subunit of viral RNA polymerase. Microbes Infect. 14, 740–747.

Zhou, Y.B., Liang, S., Jiang, Q.W., 2012. Factors impacting on progress towards elimination of transmission of *schistosomiasis japonica* in China. Parasit. Vectors 5, 275–281.